Supporting Information

Bimetallic Ni-Co Composite Anchored in Wool Ball-like Carbon Framework as High-efficiency Bifunctional Electrodes for Rechargeable Zn-air Batteries

Fantao Kong, Yu Qiao, Chaoqi Zhang, Ruijing Li, Tingting Cheng, Aiguo Kong* and Yongkui Shan*

School of Chemistry and Molecular Engineering, East China Normal University, 500 Dong chuan Road, Shanghai 200241, P. R. China.

Corresponding Author: agkong@chem.ecnu.edu.cn, ykshan@chem.ecnu.edu.cn

CONTENTS

as counter electrode and Hg/HgO or Ag/AgCl as reference electrode.

Table S1. (a) The surface composition of different catalysts and the relative content of different types of nitrogen species on N-GCTHs, N-C-900, Co@N-C, Ni@N-C and NiCo@N-C-800, 900, 1000 from the XPS analysis. (b) The relative content of Co-Nx and Ni-Nx moieties on Co@N-C, Ni@N-C and NiCo@N-C estimated from the XPS analysis.

Table S2. (a) Comparison of ORR and OER catalytic activity for the recently reported non-precious electrocatalysts in the literature; (b) Comparison of ORR catalytic activity in acidic electrolytes for recently reported non-precious electrocatalysts in the literature.

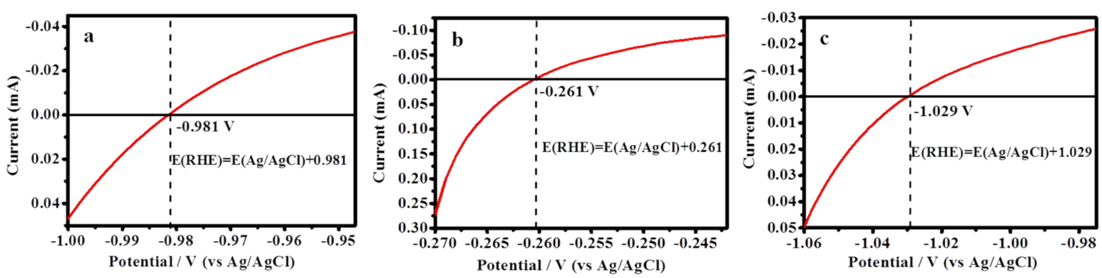

Fig. S1 Calibration to reversible hydrogen electrode (RHE) in 0.1 M KOH (a), 0.5 M H_2SO_4 (b) and 1.0 M KOH (c) electrolytes.

All the reported potentials in our paper were calibrated to the RHE potentials according to the reported method.[S1] The calibration was performed in a standard three-electrode system with platinum wires as the working and counter electrodes, and the Ag/AgCl electrode as the reference electrode. Linear scanning voltammetry (LSV) was then run at a scan rate of 5 mV s^{-1}, and the potential at which the current crossed zero is taken to be the thermodynamic potential for the hydrogen electrode reactions.

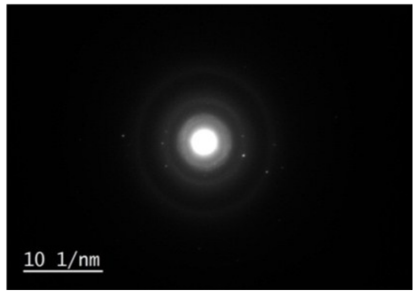

Fig. S2 The selected-area electron diffraction (SAED) image of NiCo@N-C-900.

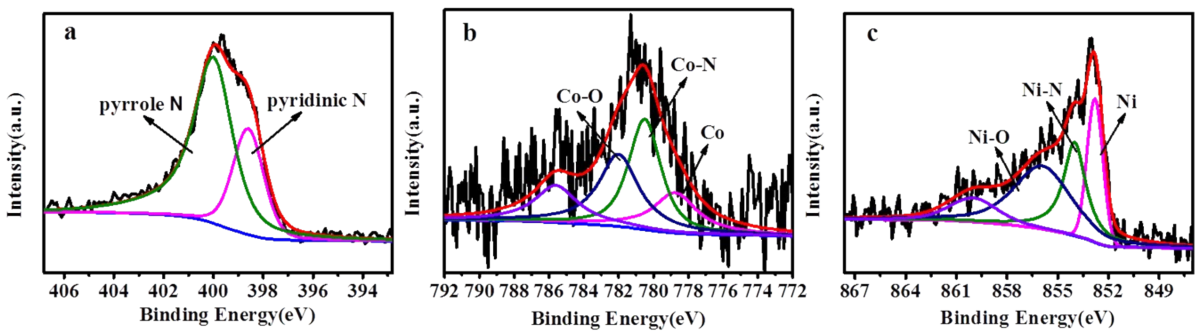

Fig. S3 (a) The high-resolution N 1s XPS spectra of the N-GCTHs, (b) Co 2p XPS spectra of the Co@N-C and (c) Ni 2p XPS spectra of the Ni@N-C.

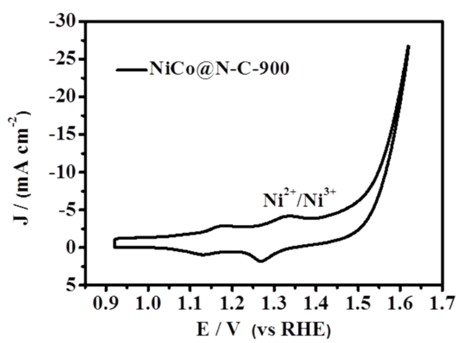

Fig. S4 The CV curve of NiCo@N-C-900 in O_2-saturated 1 M KOH solution**.**

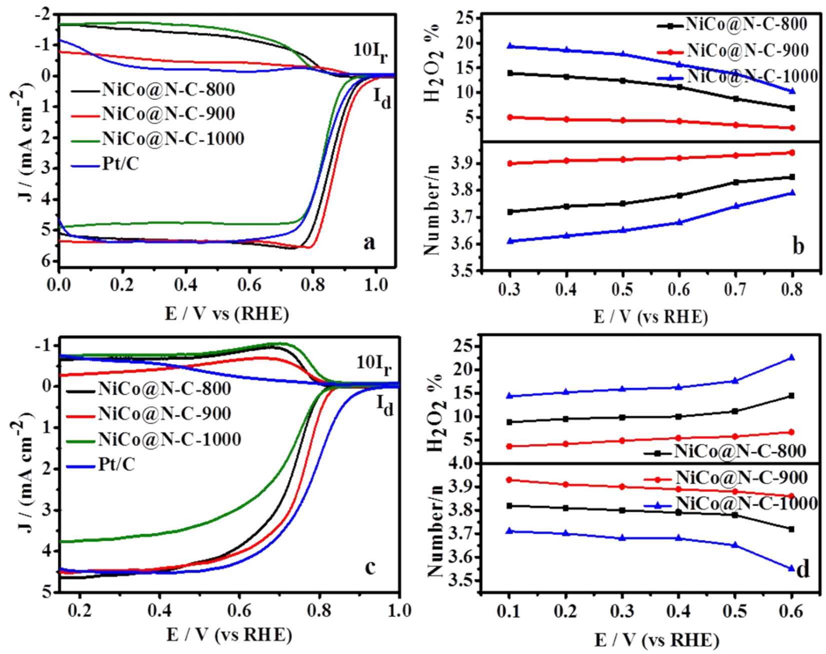

Fig. S5 (a,c) RRDE polarization curves of ORR on NiCo@N-C-800, 900, 1000 in O_2-saturated 0.1 M KOH and 0.5 M H_2SO_4 at a rotation rate of 1600 rpm. (b,d) The ORR electron transfer numbers (*n*) and yield of H_2O_2 (%) for different catalysts based on the corresponding RRDE polarization curves.

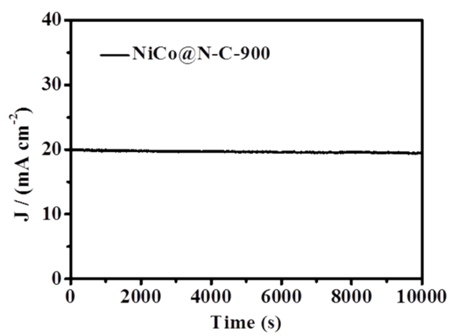

Fig. S6 Chronopotentiometric stability test of NiCo@N-C-900 with a stationary current density of 20 mA cm^{-2}.

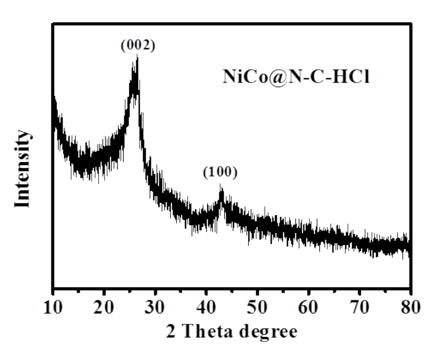

Fig. S7 XRD pattern of the NiCo@N-C-HCl catalyst.

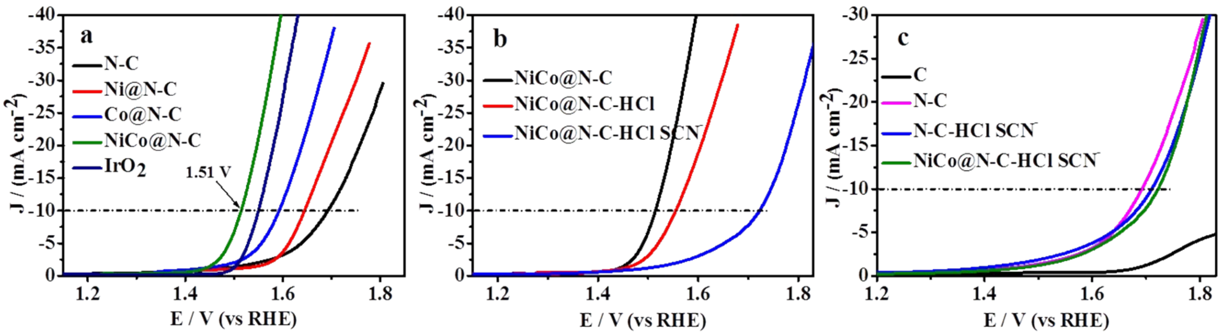

Fig. S8 (a) LSV polarization curves on N-C, Ni@N-C, Co@N-C, NiCo@N-C and IrO_2 catalysts in O_2-saturated 1.0 M KOH electrolyte. (b) LSV polarization curves of OER on NiCo@N-C, NiCo@N-C-HCl and NiCo@N-C-HCl SCN^- catalysts in O_2-saturated 1.0 M KOH electrolyte. (c) LSV polarization curves of OER on C, N-C, N-C-HCl SCN^- and NiCo@N-C-HCl SCN^- catalysts in O_2-saturated 1.0 M KOH electrolyte.

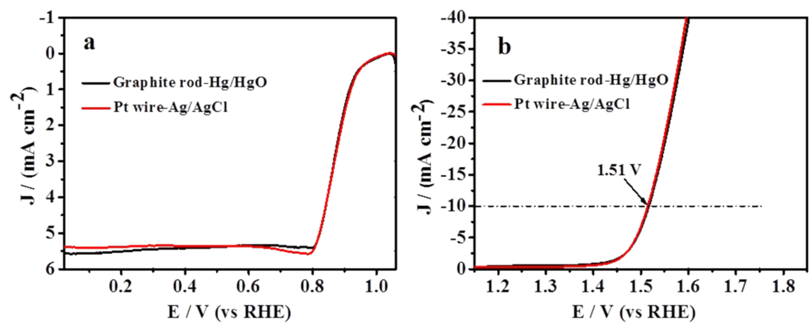

Fig. S9 The LSV curves of NiCo@N-C-900 for ORR (a) and OER (b) using graphite rod or Pt wire as counter electrode and Hg/HgO or Ag/AgCl as reference electrode.

The corresponding contrast experiments were carried out to investigate the electrocatalytic activity of NiCo@N-C-900 catalyst for ORR and OER using a graphite rod as the counter electrode and Hg/HgO as a reference electrode. As can be seen from Fig. S9-a and b, the difference of ORR and OER activity on NiCo@N-C-900 catalyst using graphite rod as counter electrode and Hg/HgO as reference electrode from that using Pt wire as counter electrode and Ag/AgCl as reference electrode is negligible in alkaline media. This result confirms that Pt can be served as the counter electrode and Ag/AgCl electrode is also stable and suitable in alkaline media. In addition, it is the most common method that Pt electrode served as a counter electrode and Ag/AgCl as a reference electrode during ORR and OER tests in alkaline media in the literature.[S2-S7]

Table S1-a. The surface composition of different catalysts and the relative content of different types of nitrogen species on N-GCTHs, Co@N-C, Ni@N-C and NiCo@N-C from the XPS analysis.

Samples	Element composition (at. %)					Relative content (%)				
	C	N	O	Co	Ni	Py-N	M-N_x	Pyr-N	G-N	NO_x
N-GCTHs	78.46	8.64	12.9	—	—	36.0	—	64.0	—	—
Co@N-C	94.23	2.39	2.87	0.51	—	15.6	24.6	15.5	23.8	20.6
Ni@N-C	93.55	1.82	2.82	—	1.8	9.1	21.8	18.5	27.4	23.2
NiCo@N-C	88.84	3.65	4.80	1.19	1.52	25.4	32.0	12.4	16.8	13.3

Table S1-b. The relative content of Co-N_x and Ni-N_x moieties on Co@N-C, Ni@N-C and NiCo@N-C estimated from the XPS analysis.

Samples	Relative content (%)		
	Co@N-C	Ni@N-C	NiCo@N-C
Co-N_x (%)	33.7	—	44.8
Ni-N_x (%)	—	23.5	32.7

Table S2-a. Comparison of ORR and OER catalytic activity in alkaline electrolytes for recently reported non-precious electrocatalysts in the literature.

Catalysts	Loading mg/cm^2	ORR Onset potential (V vs. RHE)	ORR Half-wave potential (V vs. RHE)	OER Potential at 10mA cm^{-2} (V vs. RHE)	Ref
Co@NCNT	0.425	1.03	0.828	1.66	S8
Co@Co_3O_4/NC	0.21	—	0.8	1.65	S9
NiCo@NCNT-700	0.21	0.93	0.82	—	S10
NiCo@NC	0.40	—	0.81	1.76	S11
NPCN/NiCo-NCNT	0.714	0.94	~0.87	1.59	S12
NiCo@NCNT/NF	8.45	0.97	0.87	1.54	S13
Co-C_3N_4/CNT	0.41	0.90	—	1.61	S14
NiCo/PFC	0.13	0.92	0.76	1.63	S15
NCNT/CoONiO-NiCo	0.21	1.0	0.83	1.51	S16
CuCo@NC	0.18	0.96	0.88	—	S17
PPy/FeTCPP/Co	0.30	1.01	0.86	1.57	S18
$Fe_{0.3}Co_{0.7}$/NC	0.26	—	0.88	—	S19
3D-CNTA	0.41	0.95	0.81	1.59	S20
Pt/C-JM	0.10	1.04	0.84	—	This work
NiCo@N-C-900	0.61	1.06	0.88	—	This work
	0.96	—	—	1.51	

Table S2-b. Comparison of ORR catalytic activity in acidic electrolytes for recently reported non-precious electrocatalysts in the literature.

Catalysts	Loading mg/cm^2	Half-wave potential (V vs. RHE)	Electrolytes	Ref
PPy/FeTCPP/Co	0.30	0.72	0.1M $HClO_4$	S18
NiCo@NCNT-700	0.21	0.40	0.1M $HClO_4$	S11
Co-N_x-C	0.60	0.71	0.1M $HClO_4$	S21
FeCo/C-800	0.60	0.75	0.1M $HClO_4$	S22
CoFe-PDAP	0.50	0.73	0.5M H_2SO_4	S23
PpPD–Fe–C	0.90	0.72	0.5 M H_2SO_4	S24
FePc-Py-CNT	0.32	0.66	0.5M H_2SO_4	S25
Co corrole/BP2000	0.40	0.73	0.5M H_2SO_4	S26
Co, N-CNF	0.36	0.67	0.5M H_2SO_4	S27
Fe_3Mn–AAPyr	0.60	0.75	0.5M H_2SO_4	S28
FeMo-C/N-3	0.10	0.67	0.5M H_2SO_4	S29
PANI-FeCo-C	0.60	0.80	0.5M H_2SO_4	S30
CoP-CMP800	0.60	0.64	0.5M H_2SO_4	S31
Fe/Co-CMP-800	0.60	0.78	0.5M H_2SO_4	S32
Pt-JM	0.10	0.78	0.5M H_2SO_4	This work
NiCo@N-C-900	0.81	0.76	0.5M H_2SO_4	This work

References

[S1] Y. Liang, Y. Li, H. Wang, J. Zhou, J. Wang, T. Regier and H. Dai, *Nat. Mater.*, 2011, **10**, 780.

[S2] A. Mathur and A. Halder, *Catal. Sci. Techn.*, 2019, **9**, 1245-1254.

[S3] X. Chen, J. Wang, X. Huang, X. Zhao, P. Liu, B. He, T. Wang and J. Masa, *Catal. Sci. Techn.*, 2018, **8**, 1104-1112.

[S4] H. Fan, H. Liu, X. Hu, G. Lv, Y. Zheng, F. He, D. Ma, Q. Liu, Y. Lu and W. Shen, *J. Mater. Chem. A*, 2019, **7**, 11321-11330.

[S5] P. Xi, S. Xi and J. Wang, *J. Mater. Chem. A*, 2019. *DOI: 10.1039/c9ta02894c.*

[S6] K. P. Singh, E. J. Bae and J.-S. Yu, *J. Am. Chem. Soc.*, 2015, **137**, 3165-3168.

[S7] T. D. Thanh, N. D. Chuong, H. V. Hien, N. H. Kim and J. H. Lee, *ACS Appl. Mater. Interfaces*, 2018, **10**, 4672-4681.

[S8] E. Zhang, Y. Xie, S. Ci, J. Jia, P. Cai, L. Yi and Z. Wen, *J. Mater. Chem. A*, 2016, **4**, 17288-17298.

[S9] A. Aijaz, J. Masa, C. Rösler, W. Xia, P. Weide, A. J. Botz, R. A. Fischer, W. Schuhmann and M. Muhler, Angew. Chem. Int. Ed., 2016, **55**, 4087-4091.

[S10] L. Zeng, X. Cui, L. Chen, T. Ye, W. Huang, R. Ma, X. Zhang and J. Shi, *Carbon*, 2017, **114**, 347-355.

[S11] Y. Fu, H. Y. Yu, C. Jiang, T. H. Zhang, R. Zhan, X. Li, J. F. Li, J. H. Tian and R. Yang, *Adv. Funct. Mater.*, 2018, 28, 1705094.

[S12] Y. Hou, S. Cui, Z. Wen, X. Guo, X. Feng and J. Chen, *Small*, 2015, **11**, 5940-5948.

[S13] W. Niu, S. Pakhira, K. Marcus, Z. Li, J. L. Mendoza-Cortes and Y. Yang, *Adv. Energy Mater.*, 2018, 1800480.

[S14] Y. Zheng, Y. Jiao, Y. Zhu, Q. Cai, A. Vasileff, L. H. Li, Y. Han, Y. Chen and S.-Z. Qiao, *J. Am.*

Chem. Soc., 2017, **139**, 3336-3339.

[S15] G. Fu, Y. Chen, Z. Cui, Y. Li, W. Zhou, S. Xin, Y. Tang and J. B. Goodenough, *Nano Lett.*, 2016, **16**, 6516-6522.

[S16] X. Liu, M. Park, M. G. Kim, S. Gupta, G. Wu and J. Cho, *Angew. Chem. Int. Ed.*, 2015, **54**, 9654-9658.

[S17] M. Kuang, Q. Wang, P. Han and G. Zheng, *Adv. Energy Mater.*, 2017, **7**, 1700193.

[S18] J. Yang, X. Wang, B. Li, L. Ma, L. Shi, Y. Xiong and H. Xu, *Adv. Funct. Mater.*, 2017, **27**, 1606497.

[S19] B. Y. Guan, Y. Lu, Y. Wang, M. Wu and X. W. Lou, *Adv. Funct. Mater.*, 2018, **28**, 1706738.

[S20] S. Wang, J. Qin, T. Meng and M. Cao, *Nano Energy*, 2017, **39**, 626-638.

[S21] A. Kong, Y. Kong, X. Zhu, Z. Han and Y. Shan, *Carbon*, 2014, **78**, 49-59.

[S22] Q. Lin, X. Bu, A. Kong, C. Mao, F. Bu and P. Feng, *Adv. Mater.*, 2015, **27**, 3431-3436.

[S23] Y. Zhao, K. Watanabe and K. Hashimoto, *J. Am. Chem. Soc.*, 2012, **134**, 19528-19531.

[S24] Y. Zhu, B. Zhang, X. Liu, D. W. Wang and D. S. Su, *Angew. Chem. Int. Ed.,* 2014, **126**, 10849-10853.

[S25] R. Cao, R. Thapa, H. Kim, X. Xu, M. G. Kim, Q. Li, N. Park, M. Liu and J. Cho, *Nat. Commun.*, 2013, **4**, 2076.

[S26] N. Levy, A. Mahammed, M. Kosa, D. T. Major, Z. Gross and L. Elbaz, *Angew. Chem. Int. Ed.*, 2015, **54**, 14080-14084.

[S27] L. Shang, H. Yu, X. Huang, T. Bian, R. Shi, Y. Zhao, G. I. Waterhouse, L. Z. Wu, C. H. Tung and T. Zhang, *Adv. Mater.*, 2016, **28**, 1668-1674.

[S28] A. Serov, M. H. Robson, M. Smolnik and P. Atanassov, *Electrochim. Acta*, 2012, **80**, 213-218.

[S29] L. Lin, Z. K. Yang, Y.-F. Jiang and A.-W. Xu, *ACS Catal.*, 2016, **6**, 4449-4454.

[S30] G. Wu, K. L. More, C. M. Johnston and P. Zelenay, *Science*, 2011, **332**, 443-447.

[S31] Z. S. Wu, L. Chen, J. Liu, K. Parvez, H. Liang, J. Shu, H. Sachdev, R. Graf, X. Feng and K. Müllen, *Adv. Mater.*, 2014, **26**, 1450-1455.

[S32] S. Brüller, H.-W. Liang, U. I. Kramm, J. W. Krumpfer, X. Feng and K. Müllen, *J. Mater. Chem. A*, 2015, **3**, 23799-23808.